



ASSESSMENT ON THE RELATIONSHIP OF SPECTRAL INDICES WITH LAND SURFACE TEMPERATURE USING GOOGLE EARTH ENGINE: A CASE STUDY OF CHITWAN DISTRICT, NEPAL

Bishal KHATRI^{1*} Rakshya KHATRI¹

¹ Department of Geomatics Engineering, Kathmandu University, Nepal.

* Corresponding Author: B. Khatri, ✉ bishalkhatri675@gmail.com  0009-0008-7132-6346

ABSTRACT

Land surface temperature (LST) is a significant characteristic that influences the Earth's climate system and the flow of energy between land and atmosphere. Land cover variations, as measured by spectral indices, have a substantial influence on LST. This study uses Google Earth Engine (GEE) to analyze the link between LST and several spectral indices in Nepal's Chitwan area. Chitwan was chosen for its diversified scenery, which includes thick forest within Chitwan National Park, permanent water bodies, urban areas, and continuous urbanization with rising temperatures. Landsat 8 data were used to generate the Normalized Difference Built-up Index (NDBI), Normalized Difference Water Index (NDWI), Enhanced Vegetation Index (EVI), Normalized Difference Bareness Index (NDBaI), and LST. All data collecting, processing, and extraction were done using the GEE platform. The spatial analysis discovered considerable changes in LST across the district, ranging from 18.86°C in vegetated regions to 40.69°C in urban centers and bare fields. The distribution of spectral indices revealed additional information: high EVI values indicated healthy vegetation, whereas high NDBI values linked to built-up regions. The NDWI successfully mapped water bodies, whereas NDBaI found regions with little vegetative cover. Pearson's correlation analysis supported the predicted relationships: lower LST with vegetation and water (EVI, NDWI: negative correlation), and higher LST with built-up areas (NDBI: positive correlation). This research emphasizes the use of remote sensing for analyzing land cover-LST interactions, as well as the role of plant cover in moderating urban heat island impacts.

Keywords: Land Surface Temperature, NDBI, NDWI, EVI, NDBaI.

Cited As:

Khatri, B., & Khatri, R. (2024). Assessment on the relationship of spectral indices with land surface temperature using Google Earth Engine: a case study of Chitwan District, Nepal, *Advances in Geomatics*, 2(2), 74-87. <https://doi.org/10.5281/zenodo.14555495>

INTRODUCTION

Remote Sensing (RS) and Geographic Information Systems (GIS) have improved the capacity of humans to see the environment through sensors and notice dynamic changes on the Earth's surface. This advancement has made it much easier for humans to detect changes both geographically and temporally across a greater area. Among the diverse applications in geoscience and natural resource management, RS and GIS are particularly adept at environmental and climatological issues (Taloor et al., 2021). The LST depicts both the surface temperature of the Earth and the temperature at the interface between the Earth's atmosphere and surface (Sood et al., 2020). In addition, people are becoming more inquisitive and conscious of climate change as a result of annual temperature increases. To estimate LST, adequate spatial and temporal data at the large scale is needed, especially with respect to land use/land cover (Polydoros et al., 2018). Because of this, geoscientists now understand that remote sensing is crucial for supplying the data required to evaluate ecosystem conditions and track changes across all geographical and temporal dimensions (Kothyari et al., 2020).

Satellite-based land surface temperature (LST) data offer comparatively significant geographic variability, high resolution, and constant and recurrent coverage of earth surface conditions on a regional or global level, as a result of the limits of in-situ observations of surface temperature worldwide (Yan et al., 2020). According to recent studies, the capacity of RS approaches to extract LST has been improved by the integration of multispectral bands (TM, ETM+, OLI, and TIRS) with the TIR bands of Landsat images. The Landsat series having a thermal band has the potential to estimate LST at a high spatial resolution (Ermida et al., 2020). For a variety of applications, including land surface emissivity, urban heat analysis, meteorology, and climatology, numerous methods have been developed to estimate LST (Guha and Govil, 2021). According to (Karakuş, 2019), the study done in the city center of Sivas and its surrounding shows that LULC changes have a direct impact on LST, which can be influenced by factors such as construction materials, the presence of green areas, and the city's unique geographical location and topography. The study found that urban built-up and bare lands have the highest LST. Seasonal conditions and the development of the urban environment influence several characteristics of LULC. A highly variable trend of LST distribution through time was observed, caused by its characteristics of urbanization and development (Gusso, et al., 2015). The LST–NDVI relationship is excessively complex because it is influenced by so many different things, including marsh, exposed rock surfaces, water bodies, sand dunes, dense vegetation, and construction materials (Qu et al., 2014). LST fluctuations in urban environments can be investigated using RS data based LULC indices (i.e., vegetation, water, and built-up). Previous research looked into the connection between urban surface characteristics and the spatial pattern of LST (Alexander, 2020). However, more research is required on a number of parameters that affect LST, including transpiration, evaporation, albedo, vegetation, land and cover fractions, and soil moisture emissivity and conditions. The need for precise and efficient temperature measurements makes thermal infrared (TIR) remote sensing of



LST an interesting subject, especially considering that field observations are expensive and restricted to specific locations (Khan et al., 2021). In context of Nepal, several studies have been conducted to analyze the LST but mostly in Kathmandu Valley, which is rapidly urbanizing area. It was found that the LST and NDBI are positively correlated which means the increase in built-up will increase the surface temperature. The vegetation and water have been found to have a negative correlation with the LST (Sarif et al., 2020). Another study by (Baniya et al., 2018), average LST increased significantly as the urban area expanded in the Kathmandu valley. It also showed that the NDVI values were seen low in recent years while NDBI values were extremely high in the core city areas. MODIS satellite datasets were used in another study in Nepal where the correlation between LST and NDVI was evaluated between 2000 and 2018. It showed that the urban LSTs were seen higher than the non-urban areas. However, the rate of increase in temperature was higher outside the central Kathmandu developed urban area (Mishra et al., 2019).

Meanwhile, Chitwan is also one of the rapidly urbanizing areas of Nepal. At the same time studies have found that the temperature of Chitwan has also been reaching new heights each year. No previous study in Chitwan was done regarding the land surface temperature and the significance of spectral indices. So, the major objective of this study is to analyze the relationship of LST with urban indices like NDBI, NDBaI, water indices like NDWI and vegetation indices like EVI. At the same time, our study tried to fill the research gap by performing the Pearson's correlation analysis between the indices and LST.

1. MATERIALS AND METHODS

1.1 Study area

The Chitwan district is situated close to the Indian border in the center of Nepal. It is well-known for the endangered great one-horned rhinoceros (*Rhinoceros unicornis*), Bengal tiger (*Panthera tigris tigris*), and other endemic species that thrive in the Terai region of Nepal's Chitwan National Park, which is designated as a World Heritage site and an important biodiversity hotspot at an elevation of 120 to 815 meters (UNESCO, 2019). It covers a total area of 952.63 square kilometers with extent approximately extending from 27.3986° N to 27.6786° N in latitude and from 83.1838° E to 84.1911° E in longitude. The population of Chitwan is around 579,984. The yearly average temperature typically ranges from around 25°C to 30°C.

Due to the rapid urbanization, increasing population and increasing temperature in Chitwan, it has been chosen as the suitable area to conduct this study.

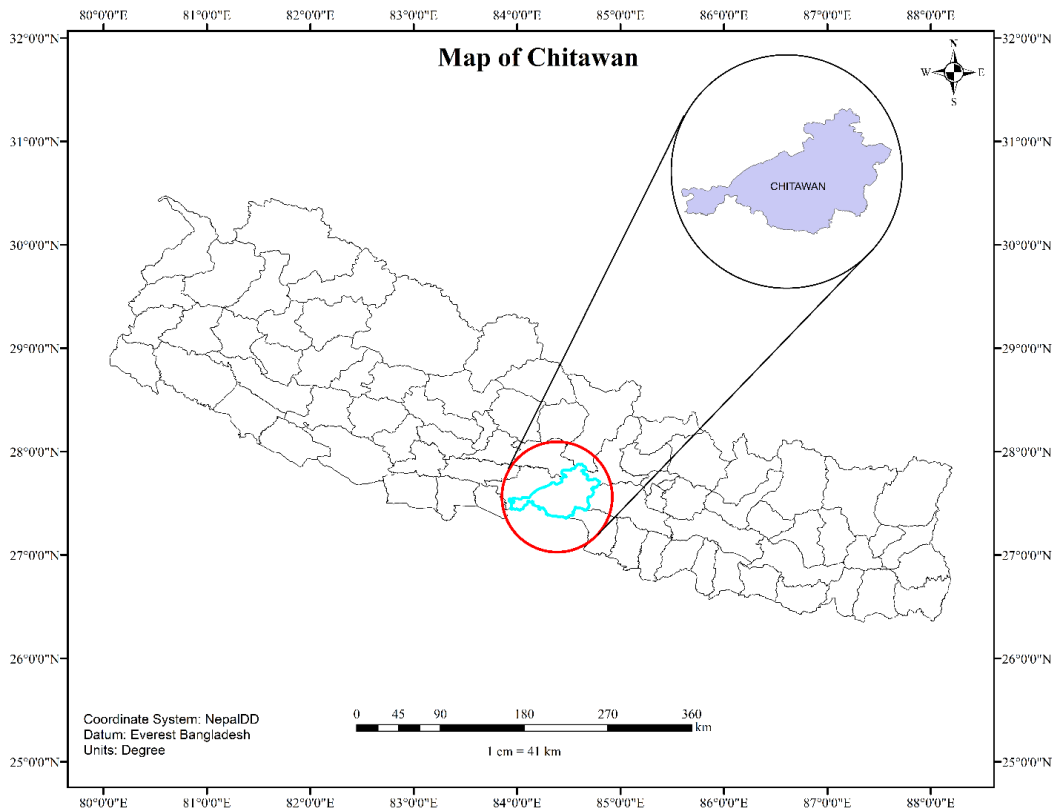


Figure 1. Study Area Map

1.2 Data Acquisition

Google earth engine was used to filter the mean Landsat 8 image between the months March and May of the year 2024. The composite image was clipped within the region of interest, which is Chitwan district. Administrative boundaries of Nepal and Chitwan were taken from the national geoportal of Nepal (source: <https://nationalgeoportal.gov.np/#/>). Cloud Masking was done in order to remove the cloudy pixels and get accurate results.

Table 1. Landsat 8 Collection 2 Tier 1 TOA image collection (Google Earth Engine. (n.d.).)

Dataset Identifier	LANDSAT/LC08/C02/T1_TOA
Platform	Landsat 8
Collection	2
Tier	1
Spatial Resolution	30 meters except B8 (15 meters)

Temporal Resolution	16 days
Spectral Bands	Band 1 (Coastal/Aerosol): 0.43 - 0.45 μm
	Band 2 (Blue): 0.45 - 0.51 μm
	Band 3 (Green): 0.53 - 0.59 μm
	Band 4 (Red): 0.64 - 0.67 μm
	Band 5 (Near Infrared): 0.85 - 0.88 μm
	Band 6 (Shortwave Infrared 1): 1.57 - 1.65 μm
	Band 7 (Shortwave Infrared 2): 2.11 - 2.29 μm
	Band 8 (Panchromatic): 0.52 - 0.90 μm
	Band 9 (Cirrus): 1.36 - 1.38 μm
	Band 10 (Thermal Infrared 1): 10.60 - 11.19 μm
	Band 11 (Thermal Infrared 2): 11.50 - 12.51 μm
Data Availability	Global
Sensor	Operational Land Imager (OLI) and Thermal Infrared Sensor (TIRS)

1.3 Land surface temperature estimation

The Land Surface Temperature was retrieved from Band 10 of the Landsat 8 image of Chitwan using the following algorithm (Mustafa et al., 2020):

$$L_{\lambda} = 0.00033442 * DN + 0.1 \quad (1)$$

Where L_{λ} is the spectral radiance in $\text{Wm}^{-2} \text{sr}^{-1} \text{mm}^{-1}$, constants 0.00033442 and 0.1 are the band-specific multiplicative and additive rescaling factor of Band 10 (thermal band) from the metadata respectively. Then the spectral radiance to at-satellite brightness temperature (TB) under the assumption of uniform emissivity. The conversion formula is given:

$$T_B = \frac{K_2}{\ln\left(\left(\frac{K_1}{L_{\lambda}}\right) + 1\right)} - 273.15 \quad (2)$$

Where, T_B is the brightness temperature in Celsius, L_{λ} is the spectral radiance in $\text{Wm}^{-2} \text{sr}^{-1} \text{mm}^{-1}$ and K_2 and K_1 are calibration constants. For Landsat-8 OLI, K_1 is 774.89 and K_2 is 1321.08.

The fractional vegetation F_v , of each pixel was determined from the NDVI using equation

$$F_v = \left(\frac{NDVI - NDVI_{\min}}{NDVI_{\max} - NDVI_{\min}} \right)^2 \quad (3)$$

d_ϵ is the effect of the geometrical distribution of natural surfaces and internal reflections calculated by:

$$d_\epsilon = (1 - \epsilon_s)(1 - F_v)F\epsilon_v \quad (4)$$

Where, ϵ_v is vegetation emissivity, ϵ_s is soil emissivity, F_v is fractional vegetation, and F is a shape factor with a mean of 0.55 (Siddique, 2021).

$$\epsilon_v = \epsilon_v F_v + \epsilon_s(1 - F_v) + d_\epsilon \quad (5)$$

Where, ϵ is emissivity, and ϵ may be determined by:

$$\epsilon = 0.004 * F_v + 0.986 \quad (6)$$

Finally, LST is calculated as

$$LST = \frac{T_B}{1 + (\lambda\sigma T_B / (hc)) \ln \epsilon} \quad (7)$$

Where, T_B is at-sensor temperature in degree Celsius, λ_σ is the average wavelength of band 10, h is Planck's constant (6.626×10^{-34}), c is the velocity of light (3×10^8 m/s) and ϵ is the emissivity calculated from Eq. 6.

1.4 Calculation of spectral indices

1.4.1 Normalized Difference Built-up Index (NDBI)

NDBI works with remote sensing data to extract, map, and monitor built-up/settlement areas. Landsat 8 OLI/TIRS was used to extract the values and map for the NDBI. Built-up and populated areas show higher reflectance in the MIR wavelength range of 1.55~ 1.75 μ m than in the NIR wavelength range of 0.76~ 0.90 μ m, in contrast to the other land cover surfaces. Range built up from (-1 to 1). The percentage of built-up regions increases with increasing built-up values. NDBI has been computed using Eq. 8 (Shah et al., 2022):

$$NDBI = \frac{SWIR - NIR}{SWIR + NIR} \quad (8)$$

1.4.2 Normalized Difference Water Index (NDWI)

The NDWI is most the appropriate index for water body mapping. Water bodies have strong absorbability and low radiation in the range from visible to infrared wavelengths. The index uses the green and NIR bands of the remote sensing images based on this phenomenon. Its values also range from -1 to +1 with values near 1 showing water bodies. It was calculated using Eq. 9 (McFeeters, 1996):

$$NDWI = \frac{Green - NIR}{Green + NIR} \quad (9)$$

1.4.3 Enhanced Vegetation Index (EVI)

The enhanced vegetation index (EVI) is an optimized vegetation index that improves sensitivity in high biomass regions and vegetation monitoring by decoupling the canopy background signal and reducing atmospheric impacts. EVI is computed according to Eq. 10 (Huete et al., 2002).

$$EVI = 2.5 * \frac{NIR - Red}{(NIR + 6 * Red - 7.5 * Blue + 1)} \quad (10)$$

1.4.4 Normalized Difference Bareness Index (NDBaI)

Normalized difference bareness index (NDBaI) is one of the most popular indices for bare land extraction that is often used in LULC and LST related studies. For Landsat 8 data, band 6 and band 10 are used as the SWIR and TIR bands, respectively. The value of NDBaI ranges between -1 and +1. Generally, the positive value of NDBaI indicates the bare land. It is given by Eq. 11 (Guha et al., 2017):

$$NDBaI = \frac{SWIR - TIR}{SWIR + TIR} \quad (11)$$

2. RESULTS

2.1 Land Surface Temperature of year 2024

Figure 2 shows that land surface temperature (LST) varies significantly over Chitwan district, ranging from a low of 18.857°C to a maximum of 40.695°C. It was estimated as the average of three months (March, April and May) of the year 2024. The warmest zones, with temperatures reaching 38°C, are mostly centered in the district's central and western areas. These places are intimately related to heavily populated metropolitan centers, such as Bharatpur metropolis, and their surrounding swaths of barren terrain. Compared to vegetated regions, urban and bare land surfaces have a higher capacity for solar radiation absorption and lesser heat retention, resulting in a significant rise in LST.

Cooler locations, with temperatures regularly below 28°C, are concentrated in the district's east and southeast. This colder zone covers the vast Chitwan National Park, which is distinguished by a dense and continuous forest canopy. This plant efficiently shades the ground, lowering solar radiation absorption and encouraging lower LST. Moving north from the National Park, the Chure Hills show a wide variety of LST values, with some parts topping 32°C and others dipping below 28°C. The fluctuation in LST within the Chure Hills can be ascribed to a number of variables. Steep slopes facing south may get more direct sunshine, resulting in greater temperatures than gentler northern slopes or valley bottoms. Furthermore, the existence of dispersed plant cover on these slopes might affect LST, with denser vegetation resulting in lower temperatures.

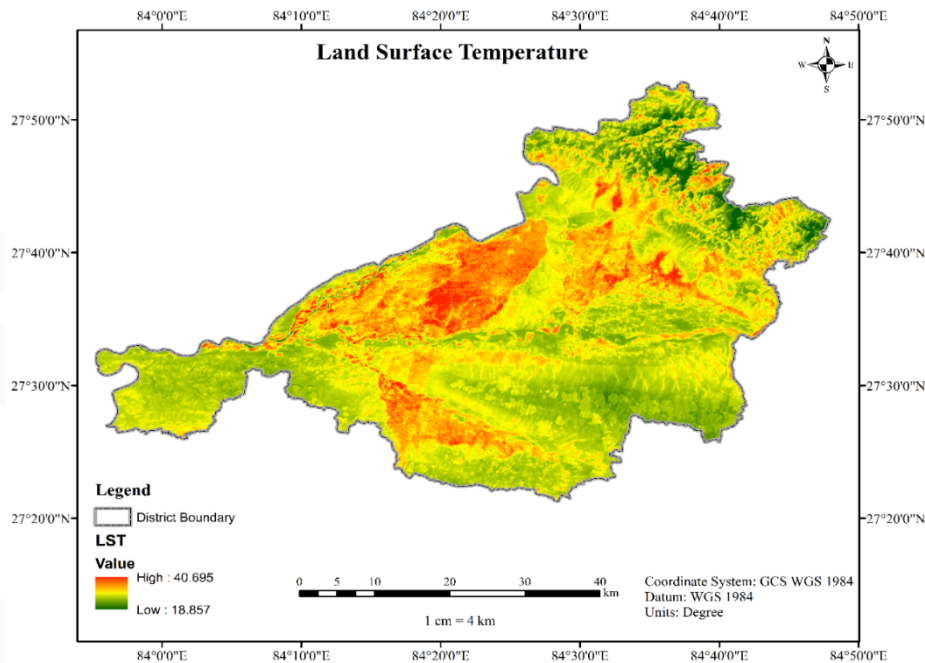


Figure 2. Land Surface Temperature Map

2.2 Spatial distribution of spectral indices

The spectral indices were calculated for the same year and months as the LST for a proper relationship assessment. The EVI map depicts the geographical distribution of vegetation health and productivity throughout the research region as shown by figure 3. Areas with EVI values greater than 0.2, particularly in the north and west, reflect healthy and thick vegetation. In contrast, lower EVI values, near -0.16, are recorded in the south and east, indicating sparser vegetation or poorer plant production. This regional pattern indicates a possible north-south or west-east gradient in vegetation health. The NDBI map in figure 4 displays the geographical distribution of built-up areas in the research region. High NDBI values above 0.35, centered in the central and southeastern regions, are most likely indicative of highly populated areas with a significant presence of structures and infrastructure. Lower NDBI values, about -0.8, are seen in the north, west, and outskirts of the central region, suggesting places with few man-made buildings and potentially natural environments. This geographical distribution indicates a strong separation between heavily populated areas and their surrounding natural or less developed zones.

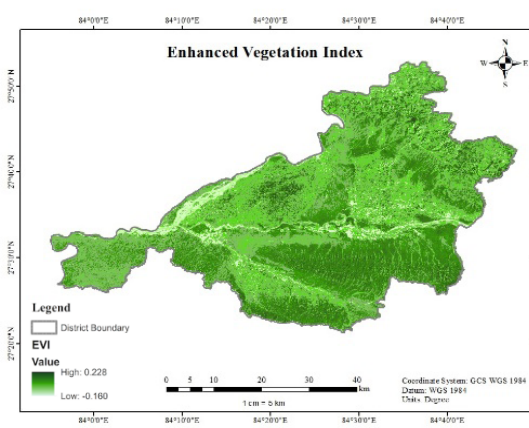
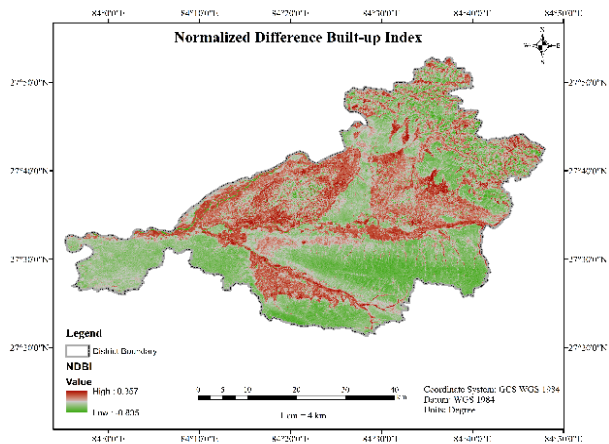
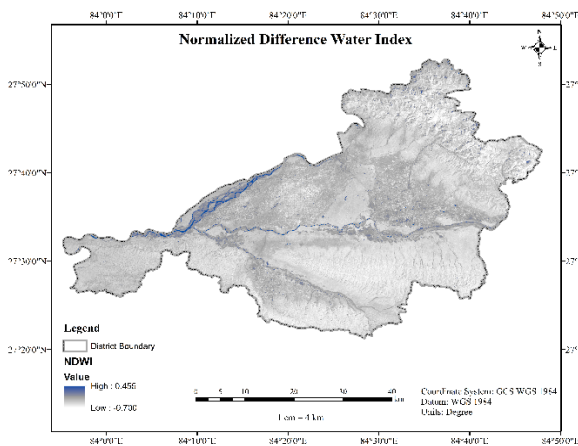
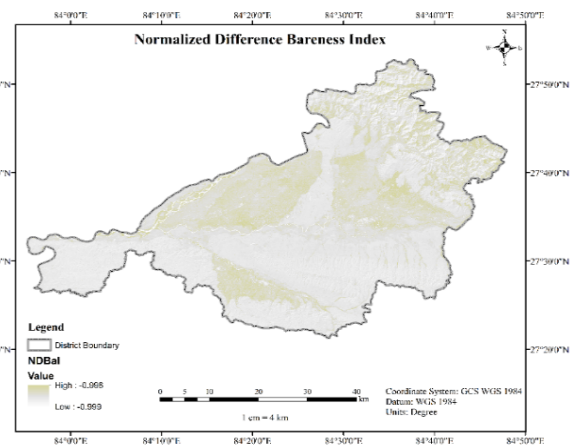
**Figure 3.** Enhanced Vegetation Index**Figure 4.** Normalized Difference Built-up Index**Figure 5.** Normalized Difference Water Index**Figure 6.** Normalized Difference Bareness Index

Figure 5 shows the Normalized Difference Water Index (NDWI) map, which illustrates the geographical distribution of water bodies in the research region. High NDWI values, more than 0.45, mainly in the center and southwest, are most likely indicative of permanent water bodies with Narayani River dominating that region. Lower NDWI values, approximately -0.7, are recorded in the north, east, and beyond the center region, suggesting that there is little to no open water. This geographical distribution distinguishes between permanent water bodies and the surrounding land characteristics. And finally, the Normalized Difference Bareness Index (NDBaI) map in Figure 6 shows the geographical distribution of barren regions within the research area. High NDBaI values, around -1, are clustered in the central and southern regions, indicating places with little plant cover, maybe barren ground, rocks, or urban areas. In contrast, lower NDBaI values (approximately -0.99) are recorded in the north, east, and periphery of the central region, suggesting places with more plant cover. This geographical pattern clearly distinguishes between bare plains and the adjacent vegetation areas.

3. DISCUSSION

3.1 Correlation of different spectral indices with the LST

Several studies have investigated the effect of different spectral indices on Land Surface Temperature (LST). NDBI has been demonstrated to have a positive association with LST, showing that places with a high density of buildings (high NDBI) experience higher temperatures (Guha & Govil, 2021; Ramaiah et al., 2020). Conversely, EVI and NDWI have been connected to negative associations with LST, implying that regions with extensive flora (high EVI) and open water (high NDWI) are usually colder (Halder et al., 2021; Ramaiah et al., 2020). NDBAI may also have a positive association with LST, however the intensity of this link varies depending on the landscape (Halder et al., 2021). These findings illustrate the complicated interplay between surface features and temperature, with built-up areas trapping heat and vegetation and water bodies reducing it.

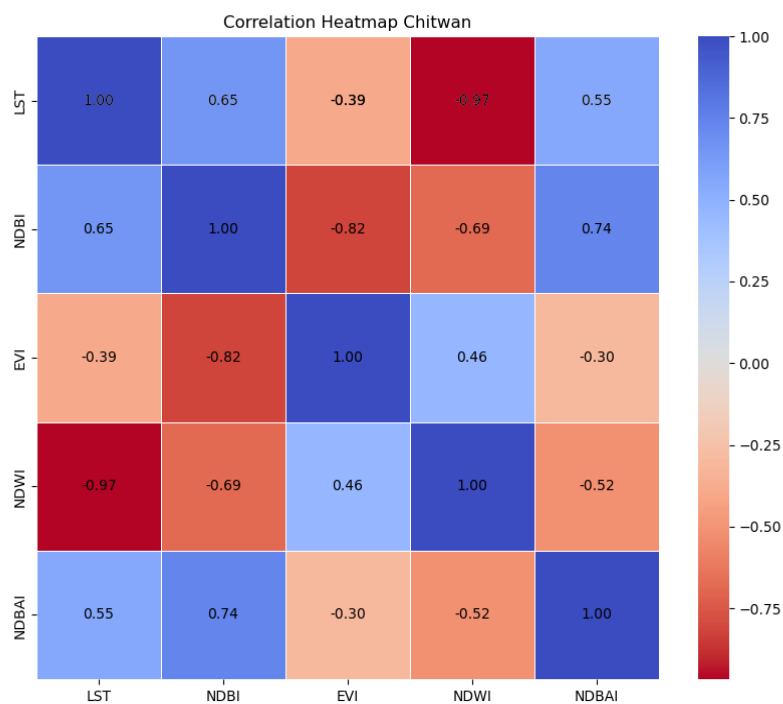


Figure 7. Correlation heatmap between LST and spectral indices

According to the heatmap obtained in this study, LST exhibited a negative correlation (-0.97) with NDWI, suggesting that areas with higher NDWI values (likely water bodies) tend to have lower LST values. A positive correlation was between LST and NDBI, with a value of 0.65. This positive correlation suggested that areas with dense built-up structures (high NDBI) were associated with higher LST. These correlations of NDBI and NDWI with LST also showed closeness in research by (Alexander,

2020), where he found that LST was negatively correlated with NDWI (-0.44), and it showed positive correlation with NDBI (0.52). There was another positive correlation (0.55) observed between LST and NDBaI, indicating a potential association between higher LST and areas with less vegetation cover (low NDBaI values). Finally, a negative correlation (-0.39) existed between LST and EVI. The result was similar in the study by (Mishra et al., 2019) where they found that LST has a negative correlation of -0.65 with the vegetation index. This implied that areas with higher EVI values (like healthy vegetation) tend to have lower LST values. (Guha & Govil, 2021) found that LST had a negative correlation with vegetation index with a value of -0.62. LST was positively correlated with both NDBI and NDBaI having values 0.71 and 0.48 respectively. However, one contrasting thing was the correlation of LST with NDWI, where LST was positively correlated to NDWI (0.23), because their study was conducted in a dry season. Overall, the heatmap highlighted the complex interplay between land cover characteristics and surface temperature, where water bodies and vegetation cover were linked to cooler temperatures, while built-up areas were associated with higher LST.

CONCLUSION

This research highlights the important correlation between land surface temperature (LST) and various spectral indices, such as NDBI, NDWI, EVI, and NDBaI, in the swiftly urbanizing context of Chitwan district. Utilizing Landsat 8 imagery alongside sophisticated remote sensing methods, our research uncovers a clear spatial pattern in which urban and bare land zones demonstrate elevated LST, whereas areas rich in vegetation and water exhibit cooler temperatures. These findings highlight the essential function of land cover in influencing surface temperatures, providing a detailed comprehension of how urban growth and environmental changes interact to affect LST fluctuations. These findings are consistent with previous studies such as (Guha & Govil, 2021), (Mishra et al., 2019), and (Ramaiah et al., 2020), which connected greater NDBI with increased LST and EVI/NDWI with lower temperatures, respectively, whereas (Halder et al., 2021) observed a varying connection of NDBaI with LST depending on landscape characteristics. The study addresses an important knowledge void by offering empirical data related to Chitwan, an area that has been inadequately examined in the analysis of LST-spectral indices.

While this study gives significant information, it does have limits. Using data from a single year limits our capacity to investigate temporal fluctuations in LST and spectral indices. Future study that uses multi-temporal data might give a more complete picture of seasonal and long-term changes. Additionally, using better resolution satellite images may allow for a more extensive investigation of specific land cover aspects within the research region. Furthermore, researching the link between LST and other environmental parameters, such as soil moisture and air temperature, may provide a more comprehensive understanding of the processes causing LST fluctuations.

REFERENCES

- Alexander, C. (2020). Normalised difference spectral indices and urban land cover as indicators of land surface temperature (LST). *International Journal of Applied Earth Observation and Geoinformation*, 86, 102013. <https://doi.org/10.1016/j.jag.2019.102013>
- Amir Siddique, M., Wang, Y., Xu, N., Ullah, N., & Zeng, P. (2021). The spatiotemporal implications of urbanization for urban heat islands in Beijing: A predictive approach based on CA–Markov modeling (2004–2050). *Remote Sensing*, 13(22), 4697. <https://doi.org/10.3390/rs13224697>
- Baniya, B., Techato, K. A., Ghimire, S. K., & Chhipi-Shrestha, G. (2018). A review of green roofs to mitigate urban heat island and Kathmandu valley in Nepal. *Appl. Ecol. Environ. Sci.*, 6(4), 137-152. <https://doi.org/10.12691/aees-6-4-5>
- Ermida, S. L., Soares, P., Mantas, V., Göttsche, F. M., & Trigo, I. F. (2020). Google earth engine open-source code for land surface temperature estimation from the landsat series. *Remote Sensing*, 12(9), 1471. <https://doi.org/10.3390/rs12091471>
- Google Earth Engine. (n.d.). Landsat_LC08_C02_T1_TOA. Retrieved from https://developers.google.com/earth-engine/datasets/catalog/LANDSAT_LC08_C02_T1_TOA
- Guha, S., & Govil, H. (2021). An assessment on the relationship between land surface temperature and normalized difference vegetation index. *Environment, Development and Sustainability*, 23, 1944-1963. <https://doi.org/10.1007/s10668-020-00657-6>
- Guha, S., & Govil, H. (2021). A long-term monthly analytical study on the relationship of LST with normalized difference spectral indices. *European Journal of Remote Sensing*, 54(1), 487-512. <https://doi.org/10.1080/22797254.2021.1965496>
- Gusso, A., Cafruni, C., Bordin, F., Roberto Veronez, M., Lenz, L., & Crija, S. (2015). Multi-temporal patterns of urban heat island as response to economic growth management. *Sustainability*, 7(3), 3129-3145. <https://doi.org/10.3390/su7033129>
- Guechi, I., Gherraz, H., & Alkama, D. (2021). Correlation analysis between biophysical indices and Land Surface Temperature using remote sensing and GIS in Guelma city (Algeria). *Bulletin de la Société Royale des Sciences de Liège*, 90, 158-180. <https://doi.org/10.25518/0037-9565.10457>
- Huete, A., Didan, K., Miura, T., Rodriguez, E. P., Gao, X., & Ferreira, L. G. (2002). Overview of the radiometric and biophysical performance of the MODIS vegetation indices. *Remote Sensing of Environment*, 83, 195-213. [https://doi:10.1016/S0034-4257\(02\)00096-2](https://doi:10.1016/S0034-4257(02)00096-2)



- Karakuş, C. B. (2019). The impact of land use/land cover (LULC) changes on land surface temperature in Sivas City Center and its surroundings and assessment of Urban Heat Island. *Asia-Pacific Journal of Atmospheric Sciences*, 55(4), 669-684.
- Khan, M. S., Ullah, S., & Chen, L. (2021). Comparison on land-use/land-cover indices in explaining land surface temperature variations in the city of Beijing, China. *Land*, 10(10), 1018. <https://doi.org/10.3390/land10101018>
- McFeeters, S. K. (1996). The use of the Normalized Difference Water Index (NDWI) in the delineation of open water features. *International journal of remote sensing*, 17(7), 1425-1432. <https://doi.org/10.1080/01431169608948714>
- Mishra, B., Sandifer, J., & Gyawali, B. R. (2019). Urban heat island in Kathmandu, Nepal: Evaluating relationship between NDVI and LST from 2000 to 2018. *International Journal of Environment*, 8(1), 17-29. <http://dx.doi.org/10.3126/ije.v8i1.22546>
- Mustafa, E. K., Co, Y., Liu, G., Kaloop, M. R., Beshr, A. A., Zarzoura, F., & Sadek, M. (2020). Study for predicting land surface temperature (LST) using landsat data: a comparison of four algorithms. *Advances in Civil Engineering*, 2020(1), 7363546. <https://doi.org/10.1155/2020/7363546>
- Polydoros, A., Mavrakou, T., & Cartalis, C. (2018). Quantifying the trends in land surface temperature and surface urban heat island intensity in mediterranean cities in view of smart urbanization. *Urban science*, 2(1), 16. <https://doi.org/10.3390/urbansci2010016>
- Qu, C., Ma, J. H., Xia, Y. Q., & Fei, T. (2014). Spatial distribution of land surface temperature retrieved from MODIS data in Shiyang River Basin. *Arid Land Geography*, 37, 125-133.
- Ramaiah, M., Sreekanth, D. M., & Sathish Kumar, K. N. (2020). Relationship between LST and NDVI/SAVI/NDBI in Panaji and Tumkur city using landsat 8 data. *International Journal of Innovative Science and Engineering*, 7(2), 331-335.
- Sarif, M. O., Rimal, B., & Stork, N. E. (2020). Assessment of changes in land use/land cover and land surface temperatures and their impact on surface urban heat island phenomena in the Kathmandu Valley (1988–2018). *ISPRS International Journal of Geo-Information*, 9(12), 726. <https://doi.org/10.3390/ijgi9120726>
- Shah, S. A., Kiran, M., Nazir, A., & Ashrafani, S. H. (2022). Exploring NDVI and NDBI relationship using Landsat 8 OLI/TIRS in Khangarh taluka, Ghotki. *Malaysian Journal of Geosciences (MJG)*, 6(1), 08-11. <http://doi.org/10.26480/mjg.01.2022.08.11>
- Sood, V., Gusain, H. S., Gupta, S., Taloor, A. K., & Singh, S. (2021). Detection of snow/ice cover changes using subpixel-based change detection approach over Chhota-Shigri glacier, Western Himalaya, India. *Quaternary International*, 575, 204-212. <https://doi.org/10.1016/j.quaint.2020.05.016>

- Taloor, A. K., Manhas, D. S., & Kothiyari, G. C. (2021). Retrieval of land surface temperature, normalized difference moisture index, normalized difference water index of the Ravi basin using Landsat data. *Applied Computing and Geosciences*, 9, 100051. <https://doi.org/10.1016/j.acags.2020.100051>
- United Nations Educational, Scientific and Cultural Organization (UNESCO). (2019). World Heritage List. Retrieved from <http://whc.unesco.org/en/list/284>
- Yan, Y., Mao, K., Shi, J., Piao, S., Shen, X., Dozier, J., ... & Bao, Q. (2020). Driving forces of land surface temperature anomalous changes in North America in 2002–2018. *Scientific reports*, 10(1), 6931. <https://doi.org/10.1038/s41598-020-63701-5>